

## Research Article

# Optimized Transverse–Longitudinal Hybrid Construction for Sustainable Design of Welded Steel Plate Girders

Iván Negrin <sup>1</sup>, Moacir Kripka <sup>2</sup>, and Víctor Yepes <sup>1</sup>

<sup>1</sup>Institute of Concrete Science and Technology (ICITECH), Universitat Politècnica de València, Valencia 46022, Spain

<sup>2</sup>Civil Engineering Graduate Program, Federal University of Technology-Paraná, Via do Conhecimento, Km 1, Pato Branco, Paraná 85503-390, Brazil

Correspondence should be addressed to Iván Negrin; [ianegdia@doctor.upv.es](mailto:ianegdia@doctor.upv.es)

Received 23 January 2024; Revised 15 March 2024; Accepted 5 April 2024; Published 30 April 2024

Academic Editor: Cun Hui

Copyright © 2024 Iván Negrin et al. This is an open access article distributed under the Creative Commons Attribution License, which permits unrestricted use, distribution, and reproduction in any medium, provided the original work is properly cited.

I-section girders with different types of steel in the flanges and web ( $f_{yf} > f_{yw}$ , respectively) are known as transverse hybrid girders. These have proven to be more economical than their homogeneous counterparts. However, the use of hybrid configurations in the longitudinal direction of the element has yet to be studied. This paper uses optimization techniques to explore the possibility of constructing transverse and longitudinally hybrid (TLH) steel girders. The optimization objective is to minimize the manufacturing cost, including seven activities besides the material cost. The geometrically double symmetric I-girder design subjected to a uniform transverse load is performed using Eurocode 3 specifications. Nine case studies are implemented, varying the element span ( $L$ ) and the applied load. The results show that establishing various configurations along the length of the element is beneficial. The optimum number of transition points is six, meaning the girder will have four configurations, i.e., one central and three others symmetrically distributed toward each half of the element. The optimum position for the first transition would be at  $0.24^*(L/2)$ , the second at  $0.40^*(L/2)$ , and the third at  $0.60^*(L/2)$ . The optimum extreme configuration is usually homogeneous ( $f_{yf} = f_{yw} = 235$  MPa). The others increase the steel quality in the plates, maintaining hybrid arrangements to reach the central one that usually remains with S700 steel for the flanges and S355 for the web. The study shows that TLH configurations are more effective for elements with larger spans. By applying the formulated design recommendations in a different case study, the manufacturing cost dropped by over 50% compared to the traditionally designed element and by more than 10% relative to the optimized element with a homogeneous configuration. The study's limitations and encouraging results suggest future lines of research in this area.

## 1. Introduction

In recent years, there has been increasing recognition of the profound effects that human actions have on the environment, particularly in terms of climate change and the diminishing availability of natural resources. Among those responsible for this impact is the construction industry, accountable for approximately 5% of global carbon dioxide emissions and identified as one of the most resource-intensive sectors [1–3]. Recognizing this, the Brundtland Commission, in 1987, established the term “sustainable development,” defining it as a model that satisfies present needs without compromising the possibilities of future generations. In this regard, specific points have been stated to improve sustainability in the construction sector. Notably, the United Nations lists “sustainable cities and

communities” as the 11<sup>th</sup> objective among its 17 sustainable development goals [4, 5].

Structural design innovations aim to meet these objectives, facilitated by advancements in manufacturing and material technologies. It allows for stronger building materials but implies higher costs and environmental impacts [6]. Thus, optimizing this enhanced strength is a priority for designers and researchers. A frequent approach that has been gaining attention is the combination of different construction materials [7], such as steel–concrete [8, 9], concrete–plastics (composites), concrete–high strength concrete, and steel–special steels. Efforts are underway to enhance construction sustainability through the strategic utilization of various materials in structural designs [10].

Steel I-girders, widely used in construction worldwide, are subjected to different stresses in their plates when bending.

Classic strategies such as modifying only the section geometry to cope with these stresses (e.g., thicker flanges) result in heavy and ineffective girders. On the other hand, increasing the yield strength of the entire section reduces the thickness but also increases costs. Therefore, due to this difference in stresses, an effective solution is to use different types of steel for the flanges and web, resulting in transversely hybrid steel elements. As a result, using lower strength steel for the web than for the flanges can offer cost and environmental savings [11]. The hybrid ratio ( $R_h$ ) in this type of element is related to the ratio between the yield strength of the flanges and the web ( $f_{yf}/f_{yw}$ ) [10].

It is essential to highlight that the most significant standards related to this type of element, even when they refer to the use of different types of steel in the plates, only limit themselves to differentiate them in the structural equations. It is the case of AISC 360-16 [12], where, although there is a distinction in the steel elastic limit between the flanges and the web, clear guidance on implementing a hybrid section is lacking. A more explanatory standard about this phenomenon is the AASHTO [13]. Wollmann [14, 15] focussed on applying these considerations to the design of steel and composite girders, developing a methodology for hybrid elements. Another standard that provides more precise information, and on which this study is based, is Eurocode 3 [16, 17]. Some studies are based on this standard and, using other published works, propose alternatives to improve the specifications established in the standard itself [18, 19]. These considerations are summarized in [10] and combined to propose a simplified method for the design of transversely hybrid girders [20].

Even with these limitations, this topic has been developing for several years. However, there are still some gaps in the research. Several papers have focused on the structural behavior of these elements. For example, web behavior under point loads [21], fatigue tests [22], web buckling resistance [23], and more recently on failure mechanisms [24], bending behavior [25–27], experimental shear behavior [28], elements with web openings [29, 30], made by stainless steel [31], or with corrugated webs [32]. Other authors have proposed the use of predictive models such as nonlinear regression and artificial neural networks to obtain the optimal design of these elements [33]. Nevertheless, theoretical research on the advantages of this construction practice still needs to be completed, although some studies have revealed interesting information. It has been proved that transversely hybrid configurations improve the economic indexes of homogeneous I-section girders by about 10% [19]. In a numerical study on the performance of these elements as part of a composite steel and concrete bridge, it is stated that hybrid solutions are the only ones that present good indicators in the three objectives analyzed (weight, economy, and environmental impact) [11]. Though these investigations do not conduct an in-depth study on exploiting hybrid steel construction. Others have implemented optimization techniques to explore this alternative to homogeneous construction in experiments where this phenomenon is investigated in depth [20]. The results show economic

savings of up to 18% compared to the latter. Additionally, optimal solutions use configurations with  $R_h$  values close to 2. Therefore, it can be affirmed that hybridization benefits this type of constructive element.

Alternatively, just as the different elements of this type of structure are not subjected to the same stresses in the transverse plane, there are also differences in the longitudinal direction. If using different materials is satisfactory in the first case, it can be assumed that the same is true in the second. Several studies have investigated the advantages of establishing differences in material configurations along the structural elements. For example, using different types of concrete in long-span hybrid bridge girders improves economic, environmental, and constructability indexes [34]. Significant enhancements in the structural response of the system are also obtained. Multimaterial topological optimization techniques have also been used to propose an innovative design of long-span steel–concrete composite bridges [35]. This proposal improves technical and economic indicators compared to other typical bridge types. Others have pursued an approach aimed at determining the optimal length of the steel portion within the main span of steel–concrete hybrid girder bridges [36]. Several studies have focused on one of the problems arising from hybrid construction: the joints, e.g., the behavior of longitudinal steel–concrete joints in composite steel–concrete hybrid girder bridges [37], the steel-to-concrete connection in longitudinally hybrid elements [38], the performance of joints in spliced steel–PSC hybrid girders [39, 40], or the mechanical behavior of steel–concrete joints in hybrid girders [41, 42].

Therefore, while the use of transversely hybrid configurations in I-section steel girders has been addressed to some extent, the combination of various types of steel in the longitudinal direction is a possibility that has yet to be explored. For this reason, the main objective of this study is to take as a reference the methodology proposed in previous research on the optimization of transversely hybrid girders [20] and to implement transverse–longitudinally hybridization (TLH) to enhance the previous results further. To this end, aspects that help to understand the behavior of TLH girders better and to extrapolate the results to practice will be studied in depth. The number of transitions (or points where the element changes the material properties) and their positioning are of relevant importance. Another essential point is the steel configuration for each resulting span. With these data, it is aimed to establish design recommendations for constructing this type of structure. In addition, based on the proposed methodology (with its strengths and limitations) and the results achieved, it is intended to establish a series of guidelines for future research. On the other hand, considering the immense number of possible solutions that can be given to the design of a TLH girder, applying mathematical optimization is an indispensable alternative. Then, the design procedure is formulated as an optimization problem to meet the standards' regulations in the form of constraints while improving specific indicators of the structure. The goal is to minimize the manufacturing cost, which includes seven other activities in

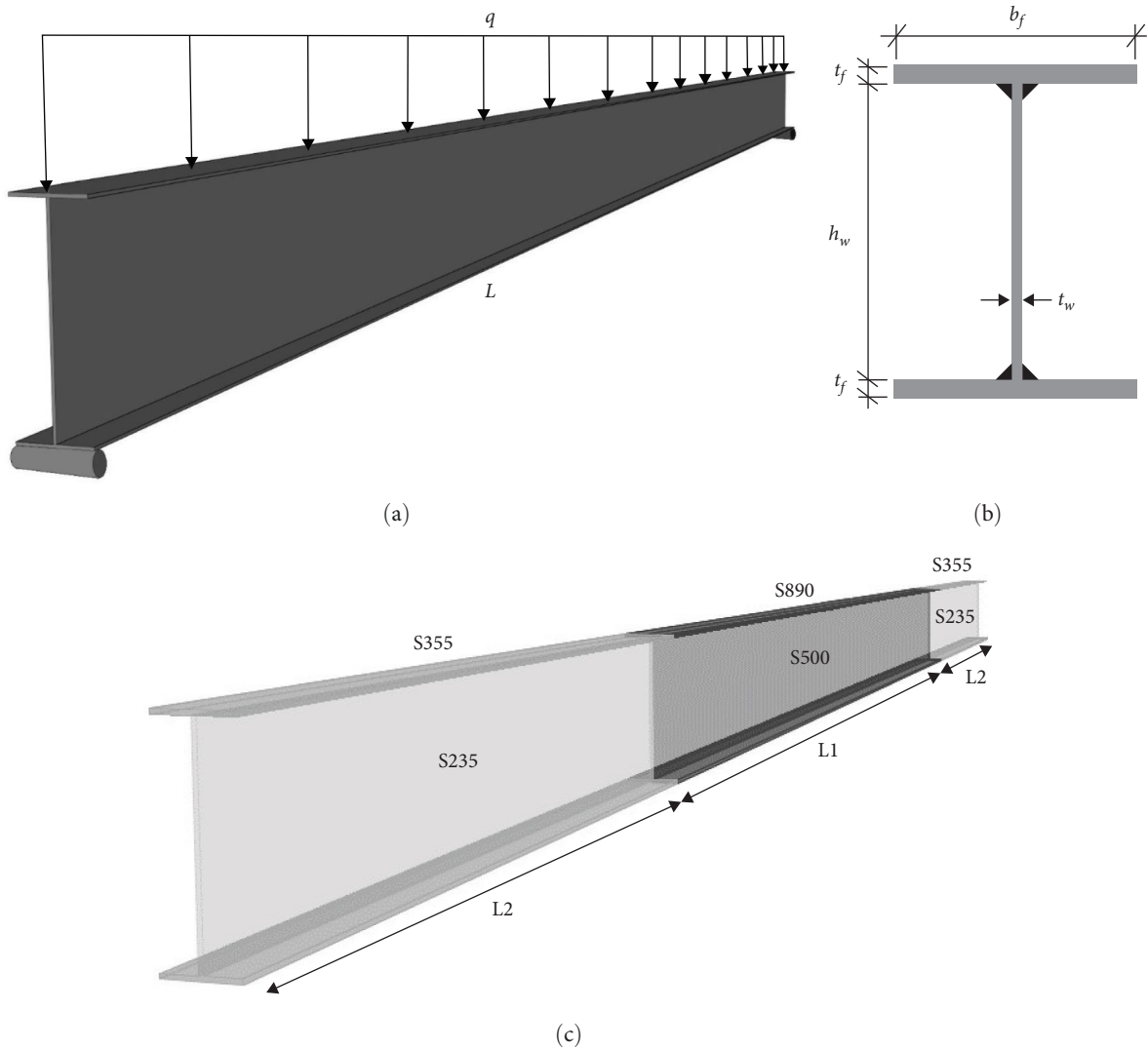


FIGURE 1: (a) Basic case study [20], (b) transversal geometric design variables, and (c) example of a TLH girder with two transition points.

addition to the material cost. The constraints are based on the Eurocode 3 specifications, incorporating amendments suggested by multiple authors. Hence, it is intended to test whether TLH configurations can improve the economic indicators of I-section steel girders compared to their homogeneous and transversely hybrid counterparts through optimization strategies. Consequently, it is expected to provide more sustainable and structurally efficient alternatives to the traditional ones used in structures such as bridges or buildings.

Accordingly, the paper is organized as follows. Section 2 is devoted to explaining the methodology used in the research. Here, the basic case study is described, and the optimization problem is formulated by defining the variables, the objective function, and the constraints. Also, the strategies for solving the formulated problem are presented. Section 3 presents and discusses the results. In addition, some recommendations for constructing TLH girders are given, and future lines of research on this subject are proposed. Finally, Section 4 summarizes the most important conclusions of the study.

## 2. Methodology

The explanation of the proposed methodology begins with a description of the case studies. Here, the fundamental aspects considered to model these structures configured transversally and longitudinally hybrid are presented. Then, the optimization problem formulation is presented, where the variables that make possible the exploration of TLH configurations, the objective function, and the design constraints are defined. Lastly, the alternatives used to solve the optimization problems are posed.

*2.1. Problem Description.* The basic structure to be optimized consists of a simply supported girder of length  $L$ , as shown in Figure 1(a). It is subjected to a distributed load  $q$  since it is assumed to support a concrete slab or similar structure. In this representation, note the depiction of fork-type supports, highlighting the restriction of rotational movement around the longitudinal axis. Three values of  $L$  (12, 16, and 20 m)

and  $q$  (20, 40, and 60 kN/m) are considered to obtain the case studies. The full combination of the factors produces nine case studies. Note that the magnitude of the distributed load corresponds to values to which a similar structure may be subjected in reality. For example, a girder part of a frame building structure might carry a load of 20 kN/m, while another, part of a bridge section, might be subjected to a load of 60 kN/m. These different load states also reflect the possible spacing between girders in a more complex structure. Therefore, elements subjected to less load are less spaced, and vice versa. The modeling incorporates the self-weight of the element, acknowledging its significance. Even when supporting a slab or similar structure, it is recognized that the girder lacks adequate transverse support to dismiss lateral-torsional buckling. Thus, the analysis accounts for the reduction in bending resistance attributed to this phenomenon.

An example of a TLH girder with two transition points (TPs) is shown in Figure 1(c). Note how the basis of the configuration is transverse hybridization. Longitudinal hybridization is created by allowing the element to take different types of steel in the flanges and web in more than one portion of the element. It is essential to note that the joints between configurations are considered welded. Other types of joints, such as bolted ones, would reduce their cost even more, so the results obtained in this study can be extended to elements joined with other technologies. As a simplification, the residual stresses in the welded joints are neglected.

**2.2. Formulation of the Optimization Problem.** As already mentioned, the optimization problem is formulated in such a way as to create a wide range of solutions that develop the hybrid concept. Since there are several such configurations, there will be several formulations. The most basic is the transverse hybrid girder [20]. From here, longitudinal hybridization is implemented. Depending on each configuration, there will be a certain number of variables. Regarding the

constraints, the number of checks performed for each type of problem varies. That is, while the hybrid transverse girder is designed (according to the constraints) in the simplest way, it becomes necessary to establish more checks when introducing the transition points leading to TLH configurations. The more types of sections the element has (more TPs), the more checking of the constraints.

**2.2.1. Variables.** In formulating these problems, two basic groups of variables are inherited from the transversely hybrid girder problem. The first one belongs to those related to the geometry of the cross-section of the element (Figure 1(b)). In this group, there are four variables. The variables related to the width of the plates ( $h_w, b_f$ ) are formed in a vector  $B$  made up of 91 values. It is crucial to note that these values must be expressed in millimeters (mm) to implement the objective function and constraints correctly.

In the previous study [20], it was shown that the web height ( $h_w$ ) limitation affects the optimal mechanical distribution (geometry + material) of the solutions. The same interval should not be considered for all the study cases since some are more stressed than others. Therefore, to reach their optimum configuration, they need larger dimensions. Consequently, three different intervals are established for each element as a function of its length  $L$ . For elements of shorter length ( $L = 12$  m), the vector  $B_{12}$  will have values between 100 and 1,000 mm in 10 mm intervals (100 : 10 : 1,000). For elements of intermediate length, the vector  $B_{16}$  varies its values between 600 and 1,500 mm (600 : 10 : 1,500). For the elements of  $L = 20$  m, the values of the vector  $B_{20}$  range between 900 and 1,800 mm (900 : 10 : 1,800). Concerning the variable  $b_f$  in all cases, its values range between 100 and 1,000 mm, also in 10 mm intervals. On the other hand, the variables associated with plate thicknesses ( $t_w, t_f$ ) have a space of possible values, as shown in vector  $T$  of Equation (1) (19 values):

$$T = \{5, 6, 8, 10, 12, 14, 15, 16, 18, 20, 22, 25, 30, 35, 40, 50, 60, 80, 100\} \text{ (mm)}. \quad (1)$$

The other basic group of variables corresponds to the configuration of the material in the plates ( $f_{yw}, f_{yf}$ ). Eleven types of steels are included in the formulation, with the restriction that the yield strength of the flanges  $f_{yf}$  does not exceed twice that of the web  $f_{yw}$  [16]. The vector  $M$  denoted in Equation (2) represents the 11 possible alternatives. It should be noted that the availability of the material is ignored in this study. It is assumed that all these types of steel are

$$M = \{S235, S275, S355, S420, S450, S500, S550, S600, S700, S890, S960\}. \quad (2)$$

The simplest optimization problem that could be implemented with these six variables is formulated in [20]. It is the case of the transversely hybrid but longitudinally homogeneous girder, i.e., the same configuration along its entire

available, as it opens the possibility of enhancing the implementation of hybrid configurations. In other words, the optimization algorithm is given a more comprehensive range of solutions to obtain the optimal one. The nominal value of yield strength ( $f_y$ ) for each steel grade is used, adjusted for plate thickness according to the guidelines of EN 1993-1-1 [17]. A proportional reduction is assumed for other steel grades not explicitly listed in the table:

length. Therefore, to obtain TLH configurations, other groups of variables must be established. It should be noted that the geometric variables of the cross-section remain constant, so the element has the same geometry along its entire length.

What varies is the material's configuration and TP's position (Figure 1(c)).

Therefore, the other group of variables is associated with the position of the TPs. So far, the mentioned variables are discrete. It is the same with these variables that regulate the transitions. The TPs are located in values multiples of 5 cm (50, 100, 150, ...,  $L/2$  mm) from the element's extreme to give it a real approach. It ensures that its configuration is constructively consistent. Thus, each transition point may be located at  $((L/2)/50)-2$  number of positions ( $L$  in mm). For example, for the 12 m girder, the variables related to this aspect can take 118 values, the 16 m one a total of 158, and further instances. Remember that since the element is symmetrical, one variable is set for each of two diametrically opposed TPs. For example, in the configuration of Figure 1(c), two TPs (one for each half of the element) move symmetrically, so only one optimization variable is assigned. For the configuration with four TPs, two variables are formulated and similar. In this study, configurations with two, four, six, and eight TPs are implemented. Then, for the formulation of TLH girders, one to four additional variables are added depending on the number of TPs.

The other group of variables corresponds to the material configurations for each resulting girder span. If it is the case of the simplest TLH element (Figure 1(c)), there are two configurations (the central one and the one at the extremes), so there are four variables regulating the type of steel in the plates. If four TPs are set, there are six, and the like. These variables are also discrete.

In summary, the dimension of the vector of variables  $\mathbf{X}$  changes depending on the case study, as shown in Equation (3). Note how a subscript  $i$  is added to the "extra" variables related to the material ( $f_{yw,i}, f_{yf,i}$ ) and to the position of the transition points ( $x_i$ ). For the configuration of a longitudinally homogeneous girder ( $i=0$ ), the problem is formulated with the six basic variables. For the TLH configurations proposed in this study,  $i$  represents half of the established transition points. Therefore, if the simplest TLH configuration (two TPs) is set, the problem is formulated with nine discrete variables (four for the section geometry, two for the material configuration of the central section, one to regulate the position of the TPs, and two for the material configuration of the extremes). For the most complex configuration (eight TPs), there would be 18 discrete variables (in addition to the six basic ones, four to regulate the positions of the TPs, and eight to regulate the other four material configurations in addition to the central one). It makes the problem, in principle, challenging to solve. Note that, for the 20 m element with eight TPs, the problem would have a solution space of about  $1.19 \times 10^{26}$  possible designs. Fortunately, specific rules allow problems to be formulated much more simply. It is developed in Section 2.3:

$$\mathbf{X} = \{h_w, t_w, b_f, t_f, f_{yw}, f_{yf}, x_i, f_{yw-i}, f_{yf-i}\}. \quad (3)$$

**2.2.2. Objective Function.** The optimization objective of this study is the manufacturing cost, since in the previous study [20], it was demonstrated that it offers very different results

to such a common objective as the weight of the element. Furthermore, although the results are similar when optimizing only the material cost, there are some differences. It is because the basic manufacturing cost ( $M_B(\mathbf{X})$ ) includes, in addition to the material cost itself ( $C_M(\mathbf{X})$ ), seven other activities, as shown in Equation (4):

$$M_B(\mathbf{X}) = C_M(\mathbf{X}) + C_E(\mathbf{X}) + C_P(\mathbf{X}) + C_W(\mathbf{X}) + C_B(\mathbf{X}) + C_C(\mathbf{X}) + C_S(\mathbf{X}) + C_T(\mathbf{X})(\epsilon). \quad (4)$$

Here,  $C_E(\mathbf{X})$  represents the erecting cost,  $C_P(\mathbf{X})$  the painting cost,  $C_W(\mathbf{X})$  the welding cost,  $C_B(\mathbf{X})$  the blasting cost,  $C_C(\mathbf{X})$  the cutting cost,  $C_S(\mathbf{X})$  the sawing cost, and  $C_T(\mathbf{X})$  the transportation cost. For more information on how each of these costs is obtained, refer to the previous study [20].

The difference with the previous study is that the longitudinal hybridization requires additional joints for the girder construction. Equation (4) reflects the cost of joining the three plates to build the girder. However, to establish a TLH configuration, parts of the element must also be joined in the longitudinal direction. Therefore, the objective function is formulated as stated in Equation (5):

$$M(\mathbf{X}) = M_B(\mathbf{X}) + C_J(\mathbf{X})(\epsilon). \quad (5)$$

Here, the cost of the joints  $C_J(\mathbf{X})$  is obtained in the same way as calculated for joining the plates in Equation (4). That is, there are additional costs for cutting, sawing, blasting, and welding. This additional cost is essential as it decides whether the assumed savings of using different materials in the length of the element is so significant that it is feasible to establish the transitions.

It is needed to highlight the choice of this objective function, which includes several activities associated with the manufacturing of the element. Although it is being given an economic focus in the formulation, there is some relationship with the environmental aspect. Several works have shown that economic optimization is closely related to environmental optimization [43, 44]. Many activities included in the objective function are assumed to show similar behavior in both indicators. For example, the higher the energy consumption (more impact on the environment), the higher the cost. Therefore, it can be said that, in a certain way, the structure's sustainability is being directly improved.

**2.2.3. Constraints.** The optimization problem's constraints guarantee the correctness of the design. They are based on Eurocode 3 [16, 17]. The design methodology is based on the proposals of [18, 19, 45], adjusted according to Negrin et al. [20]. Two constraints have already been mentioned. The first one is that the yield strength of the flanges steel does not exceed twice that of the web. The other refers to the transition points, where the possibility of these points moving all over half of the element makes it necessary to restrict their positions to be correct. The first transition point must be positioned before the second, the second before the third,

and similar. The way to impose these restrictions is to check if they are fulfilled. If not, the value of the objective function is penalized. The penalty will be higher or lower depending on the number of constraint violations of a solution. The higher the number of violations, the more the objective function is penalized. It guarantees to distinguish quality within infeasible solutions.

The other major group of constraints directly relates to compliance with the strength and serviceability limit states. The check is performed at a few specific points for the longitudinally homogeneous girder. For the bending resistance, it is sufficient to take the greater value of the bending moment (at the center of the span) and check if the proposed cross-section for the whole element is resistant. In the case of shear, the highest value is found in the supports, and further instances. However, TLH configurations have several types of sections, so it is necessary to establish more checks. In this case, the moment and shear values for the ends of each configuration are taken to make the check. Since there are several sections, all of them must be checked according to their position through the element. The stiffness constraint is the same as in the longitudinally homogeneous girder since the stiffness of the sections is the same (same geometrical properties and all steels have the same modulus of elasticity  $E$ ).

(1) *Bending Resistance.* The bending resistance constraint is summarized in Equation (6). Remember that in TLH configurations, all types of sections of the element are checked. As it is symmetrical, it is worked with only one half:

$$M_{Rk}(\mathbf{X}) \geq M_{Ed}. \quad (6)$$

Here,  $M_{Rk}(\mathbf{X})$  is the bending resistance of the section, and  $M_{Ed}$  is the maximum bending moment to which it is subjected. For the central configuration,  $M_{Ed} = q_T L^2 / 8$ . Note how the subscript  $T$  is added to the distributed load term  $q$ . It means that it is the total load, including the self-weight of the element. The bending moment equation for half of the element is used to check the other sections. It provides the value of the internal force at the desired position. Refer to [20] for the complete methodology.

(2) *Lateral-Torsional Buckling.* The reduction factor for lateral-torsional buckling may reflect that used for homogeneous girders. It has to be applied to the calculated bending resistance of the cross-section following the aftermentioned rules. The reduction method is detailed in Eurocode 3-1-1 ([17], Section 6.3.2). The slenderness parameter ( $\lambda_{LT}$ ) is derived from Equation (7). Here,  $M_{cr}$  represents the critical bending moment calculated using the gross properties of the cross-section based on elastic stability theory:

$$\lambda_{LT}(\mathbf{X}) = \sqrt{M_{Rk}(\mathbf{X}) / M_{cr}}. \quad (7)$$

(3) *Shear Resistance and Buckling.* Equation (8) summarizes the shear resistance constraint. The maximum shear at the supports is  $V_{Ed} = q_T L / 2$ , although it is checked for the extreme configuration and all section types. As with the

bending moment, the shear at a given point is obtained by evaluating the position of that point in the shear equation.  $V_{c,Rd}(\mathbf{X})$  is the plastic shear resistance obtained according to Eurocode 3-1-5 ([16], Section 5):

$$V_{c,Rd}(\mathbf{X}) \geq V_{Ed}. \quad (8)$$

As per Eurocode 3-1-1 ([17], Clause 5.1(2)), the shear buckling must be considered if the ratio of  $h_w / t_w$  exceeds  $72\epsilon / \eta$ . Subsequently, transverse stiffeners must be installed at the element's supports, as stated in Clause 5.1(2) of [17] and Section 9.3 of [17].

(4) *Flange Buckling against the Web.* On the other hand, the  $h_w / t_w$  ratio must satisfy the criterion detailed in Equation (9), as specified in Clause 8(1) of [17], to prevent the compression flange buckling in the web plane. Here,  $E$  represents the modulus of elasticity of the steel (210,000 MPa),  $A_{fc}$  stands for the effective cross-sectional area of the compression flange, and the coefficient  $k$  is set at 0.40 for plastic moment resistance or 0.55 for elastic moment resistance:

$$\frac{h_w}{t_w} \leq k \frac{E}{f_{yf}} \sqrt{\frac{h_w t_w}{A_{fc}}}. \quad (9)$$

(5) *Girder Deflection.* The stiffness constraint is written as in Equation (10) since the maximum displacement ( $u_{\max}$ ) occurs at the center of the span. Note that the longitudinal hybridization does not influence the element's stiffness since all steels have the same  $E$  value. Here,  $\bar{u}$  is the maximum allowable displacement:

$$u_{\max}(\mathbf{X}) \leq \bar{u}. \quad (10)$$

Following the approach in the previous study, a frequently adopted value such as  $L/400$  is applied. The maximum displacement is determined using Equation (11), where  $q_{SLS}$  represents the serviceability limit state load (in N/mm), assumed as  $0.75q$ .  $I_y$  denotes the cross-sectional moment of inertia about the bending axis (in  $\text{mm}^4$ ):

$$u_{\max}(\mathbf{X}) = \frac{5}{384} \frac{q_{SLS} L^4}{EI_y(\mathbf{X})}. \quad (11)$$

**2.2.4. Mathematical Formulation of the Problem.** Summarizing, the problem is formulated with discrete variables. The number of these variables is different for each case study. Equation (12) represents the general formulation of the problem. Here we can see general constraints such as those on the position of the transition points ( $x_i < x_{i+1}$ ). It means that the positions of the transition points must be ordered. Therefore, no point  $x_i$  must have a position greater than the next one  $x_{i+1}$ . It is for problems with configurations of more than two TPs. In configurations of two TPs, the position of this point ranges from 0 to  $L/2$ , without being able to take any of the extreme values.

It is important to emphasize that this formulation involves solving nonlinear optimization problems. Moreover, there are specific discontinuities within the constraint functions, such as those occurring when the cross-section class changes in the bending resistance constraint. Consequently, the mathematical characteristics of these constraints pose challenges in locating the global optimum, making nonlinear discrete optimization methods impractical [20]:

$$\begin{aligned}
 & \min M(\mathbf{X}) \\
 & \text{Such that } M_{Ed} \leq M_{Rk}(\mathbf{X}) \\
 & V_{Ed} \leq V_{c,Rd}(\mathbf{X}) \\
 & \frac{h_w}{t_w} \leq k \frac{E}{f_{yf}} \sqrt{\frac{h_w t_w}{A_{fc}}} \\
 & u_{\max}(\mathbf{X}) \leq \bar{u} \\
 & f_{yf} \leq 2f_{yw} \\
 & x_i < x_{i+1} \\
 & b_f, h_w \in B \\
 & t_f, t_w \in T \\
 & f_{yf}, f_{yw} \in M.
 \end{aligned} \tag{12}$$

**2.3. Solution of the Optimization Problems.** As already established, the solution to these problems can be tricky. The complexity of optimizing the 20 m girder problem for a THL configuration with eight TPs was already mentioned. However, as we begin to solve the most straightforward problems, we discover something that makes the formulation can be significantly simplified. When optimizing the girders with TLH configurations, it was found that the optimum central section (geometry and material) was the same as that obtained when optimizing the longitudinally homogeneous element. What changed were the other configurations. Therefore, to solve the problems, it is started by optimizing the girder allowing only the transverse hybrid configuration, as was done in [20]. Once the optimal configuration has been obtained, the only thing left to optimize is the transition points' position and the other sections' material configurations. The central geometrical configuration is the same as when optimizing the longitudinally homogeneous element. Therefore, the 20 m girder problem with eight TPs would go from having 18 variables ( $1.19 \times 10^{26}$  possible solutions) to having 12 ( $3.29 \times 10^{17}$  possible solutions). In addition, the problem becomes simpler to solve by eliminating geometric variables that make the system response more complex.

Consequently, the two TPs problem is now quite simple to solve. Thus, applying a heuristic would be unnecessary. In the results section, when analyzing the behavior of TLH girders with two transitions, a rather exciting conclusion about the assumed optimal position of the two points is reached. As a result, a simple method is created. The search is started from the point while applying the proposed rule. Several moves are made in both directions until the actual optimal point is found. With this strategy, the above conclusion is validated since the optimal transition position is

undoubtedly close to the point proposed as a practical recommendation.

For the other optimization problems, the same strategy as in the previous study is used. It consists of a heuristic known as biogeography-based optimization (BBO), created by Simon [46]. This strategy has been successfully applied in discrete structural optimization problems [47]. It has been successfully used to solve the transversely hybrid girder problem. In addition, the advantages of BBO over other similar strategies to deal with this type of problem are exposed [20]. It should also be noted that the parameters that regulate the operation of the method are tuned to achieve optimum performance. The global convergence of the algorithm is verified by the extreme value theory [48].

**2.4. Data Analysis and Research Limitations.** In order to obtain and analyze the data correctly, the first step is to guarantee the best possible results, i.e., that the optimization method offers the global optimum solution, or at least one very close to it. It is well-known that heuristics are stochastic processes so that each result may differ in each optimization procedure. However, reliable data are ensured with the BBO parameter tuned (as mentioned, excellent for dealing with this type of discrete optimization problem) and the corresponding statistical analysis. Therefore, the data analysis starts with the corresponding analysis to apply the extreme value theory. It is necessary to clarify that, in most problems, this analysis is elementary because BBO converges quickly and recurrently to the best solution. Therefore, this is a potential source of error that is controlled and does not limit the scope of the results.

Once all the solutions have been obtained, the data analysis will primarily be descriptive through visualization. Tools such as line graphs, bar charts, schematic views of structural solutions, and table representations ensure the correct interpretation of the phenomenon. In some cases, these tools are accompanied by other procedures such as curve fitting, normalization of curves by averaging their data, and other mathematical operations such as scaled averaging.

Regarding the study's limitations, one of the most important is the lack of clarity in the codes regarding the design of this type of element. However, with the integration of information from Eurocode 3 and the research of several authors, the rules have been adjusted to obtain reliable methodologies. Supported by the results of applying this and other published methodologies, future work should ensure a better understanding of this type of construction, as discussed in the future research section. Therefore, based on the promising results and the new typologies that have been discovered, work in the laboratory is indispensable to refine this type of construction.

Another important limitation lies in the support conditions and load states. This research is limited to studying simply supported elements subjected to distributed loading, such as a girder part of a bridge with isostatic spans. Therefore, the results may vary in other types of structures, such as bridges with continuous spans, or elements subjected to other types of loads, such as patch loading. In addition, the study does not consider the elements supported by the structure (e.g., concrete slab), which provide stiffness to the

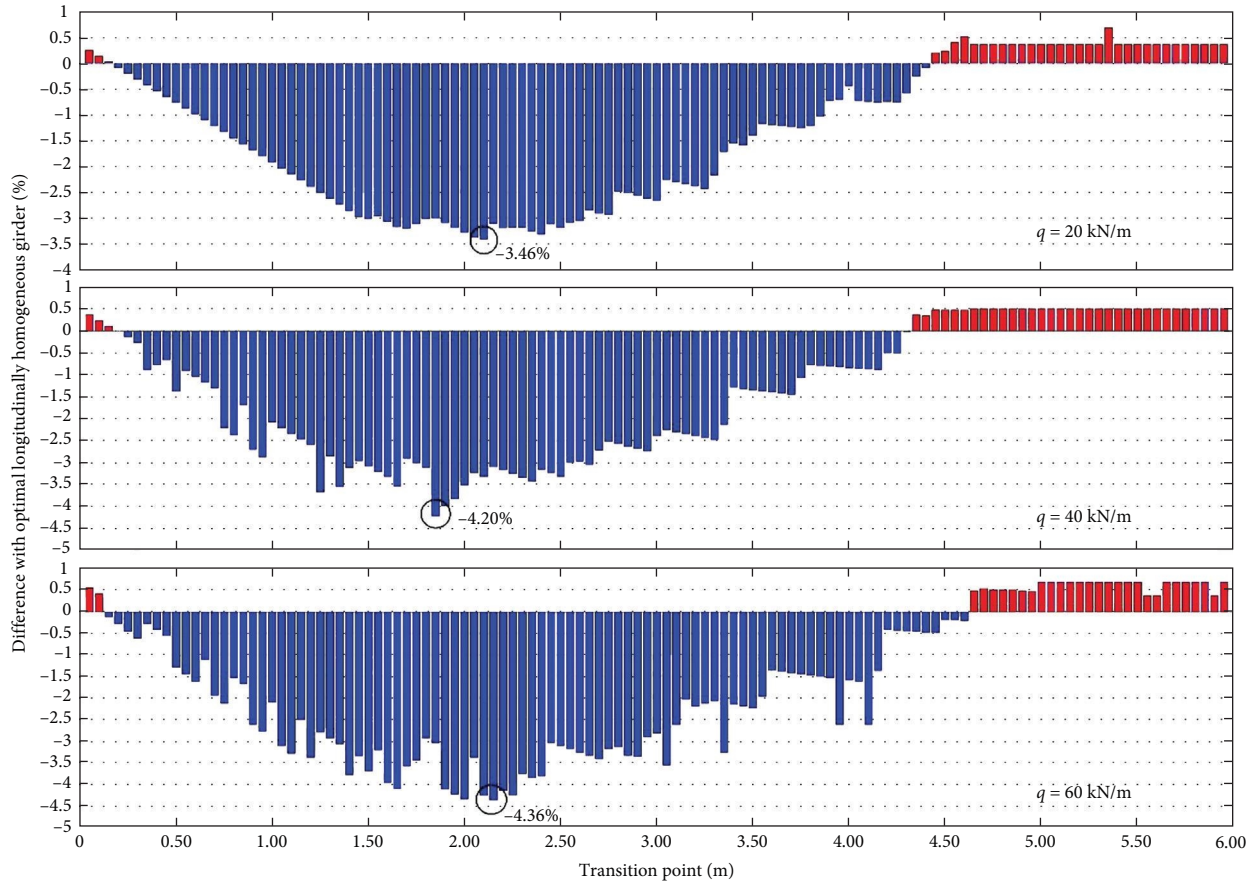


FIGURE 2: Behavior of the TLH girder manufacturing cost in comparison with the optimal cost of the transversely hybrid girder.

structure, making it more resistant. It is necessary to emphasize that keeping the structure in its simple state is of great benefit when developing and better understanding (1) the optimization problem formulated to explore and exploit the hybrid construction, and (2) the fundamental particularities of this novel construction proposal from the structural point of view. However, the methodology represented in this work perfectly applies to all these cases so that the study can be extended, and the results can be further generalized, as proposed later.

### 3. Results and Discussion

The analysis and discussion of the results are structured as follows. First, a general study of longitudinal hybridization is carried out to begin understanding the phenomenon. For this purpose, the case study of the 12 m girder is used, starting with two transition points. Subsequently, more of these points are configured to observe the element's behavior as it has more hybrid spans. Once these preliminary results have been analyzed and discussed, the proposed strategies are applied to the other case studies. With this, the results can be generalized, and conclusions can be drawn about the behavior and advantages of hybrid girders both transversely and longitudinally. Thus, the main practical recommendations for constructing TLH steel elements are summarized from the results obtained. These recommendations are applied to compare the results with a girder traditionally designed, a

homogeneous girder, and a transverse hybrid girder. Finally, some comments on future lines of research are developed.

**3.1. Study Implementing Two Transition Points.** A girder with three configurations along its entire length (as shown in Figure 1) is obtained with two transition points. The first procedure consists of discretely varying the position of the transition point and optimizing the problem to obtain the minimum manufacturing cost. We refer to a transition point because the other one varies symmetrically. Note that the problem has eight variables, four for the geometrical configuration of the section, two for the types of steel in the central configuration, and another two for the configuration of the extremes.

Figure 2 shows the results of applying this procedure to the 12 m long girder. Each bar represents the cost comparison if the configurations are optimized by placing the transition point at that position. Note that only one half is shown since the other half is symmetrical. It can be seen how there are parts where it is not economical to make a transition (bars in red) since no benefit is achieved with longitudinal hybridization, while the additional costs of the joints are present. As can be appreciated, introducing two transition points in the element tends to be more effective as the element is more stressed. The figure highlights the optimum point for making the transition and the savings of creating a longitudinally hybrid element by changing the steel configurations at that point. For a load of  $q = 20$  kN/m, the saving is 3.46%, for



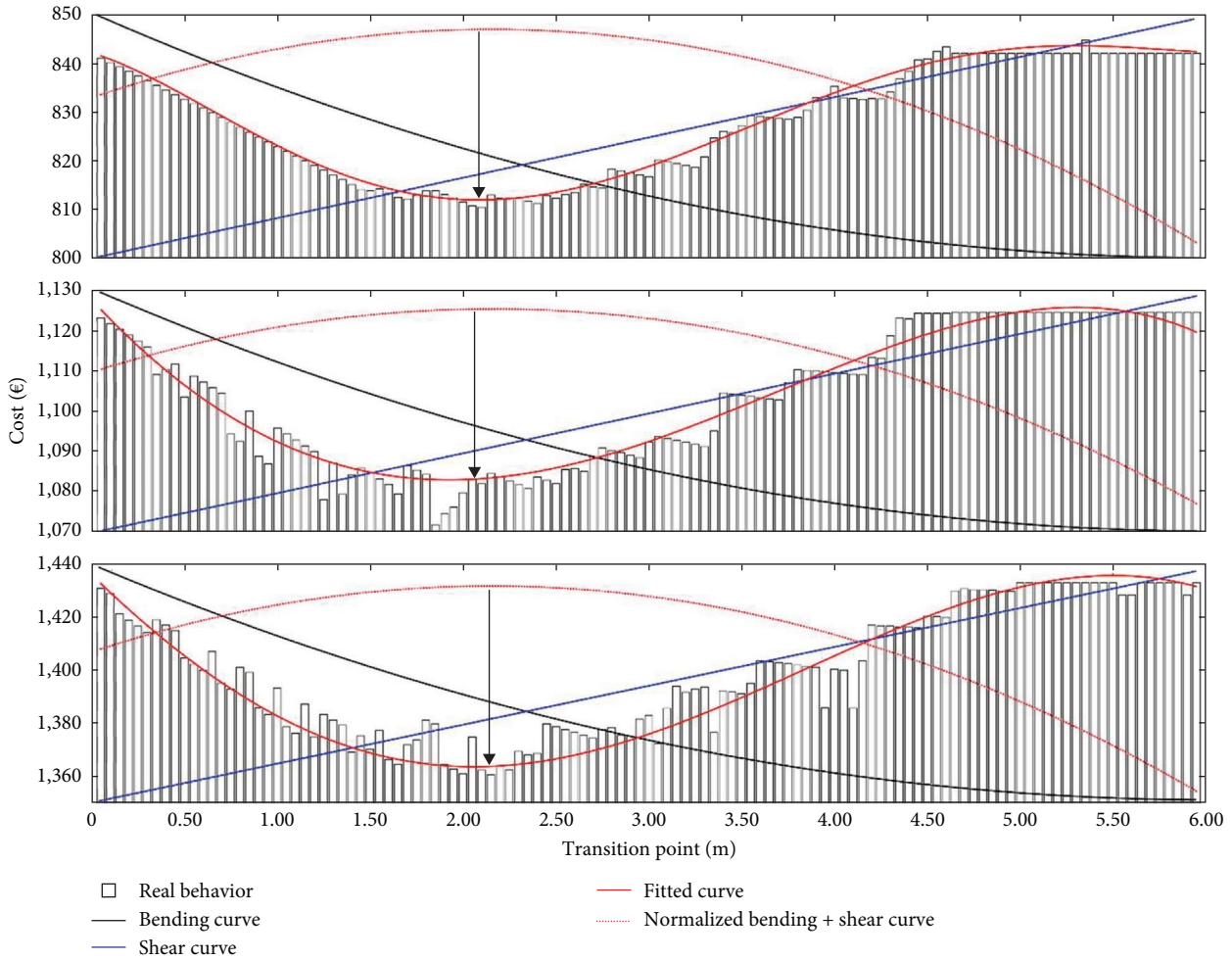


FIGURE 3: Optimal cost behavior of each case study ( $L = 12$  m) as a function of the location of the transition point.

$q = 40$  kN/m, it is 4.20%, and finally, for  $q = 60$  kN/m, it amounts to 4.36%. One might already think that longitudinal hybridization is more effective for more stressed elements.

It is important to highlight that the optimum geometrical configuration coincides with the one obtained when optimizing the element with hybrid configuration only transversal. Also, the configuration of the material in the center is the same. That is, it is obtained an element with the same cross-section and the same transverse hybrid configuration in the center as when optimizing the element only with transverse hybridization. Evidently, what changes is the extreme configuration, where the quality of the steel in the plates is reduced. Though, maintaining a hybrid configuration, i.e.,  $f_{yw} < f_{yf}$ . It helps to formulate optimization problems with more transition points in a simpler way since it is not necessary to include the geometrical variables. Only the position of the points and the material configurations for each girder span (except the central one) would be defined as variables. In other words, it is sufficient to optimize the longitudinally homogeneous element and keep the obtained configuration as the central one when optimizing the TLH element. It makes the problems much easier to solve. Evidently, it has been checked by implementing more transition points, and

the result is the same: The configuration of the most stressed part (the central one) is the same as the one obtained by optimizing the element with only transverse hybridization.

Another aspect of relevance is the reason for the optimal location of the transition point. Figure 2 shows that this position is similar for all three cases. This location would be of great practical interest when constructing hybrid girders with only two transition points. It could happen that, in practice, creating several transition points would not be feasible. In that case, using three configurations (the central one and the one at the two extremes) could improve the economic index by up to 5%. Then, knowing where to place the transition would be very productive. The other benefit is that knowing that point, a simple optimization method can be created to find the exact optimal point and the configurations to implement, as developed in Section 2.3.

The position of this transition point must be strongly related to the curves of the internal forces of the element, which regulate its design. Given the optimal location of these points, the first test was to compare them with the intercept of the bending and shear curves, which are well-known to have opposite behaviors for this type of simply supported structure. As shown in Figure 3, this crossover point is close

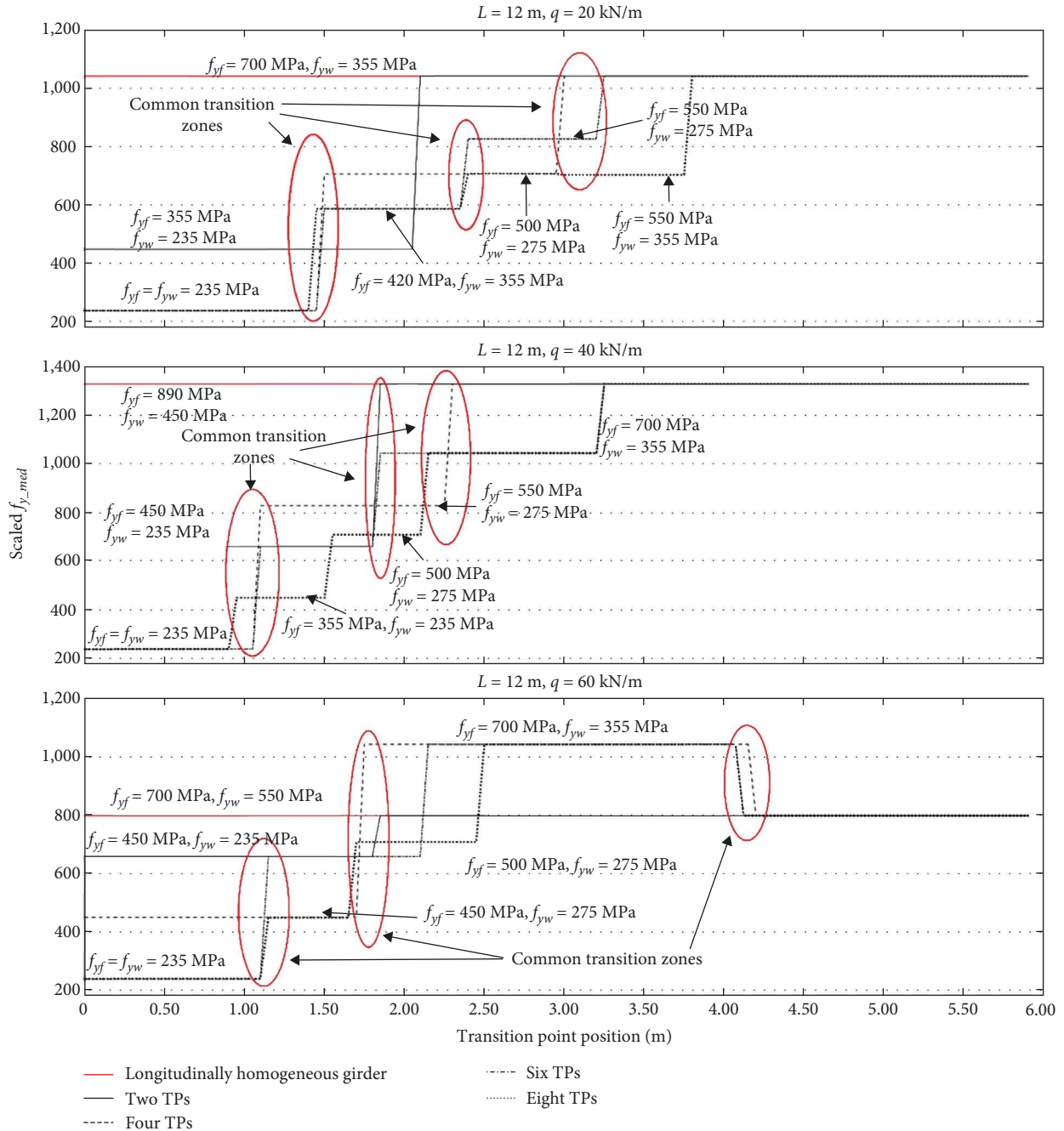


FIGURE 4: Optimal position of the transition points and material configuration for each longitudinal hybrid section. For each span section, the steel configuration of the plates is measured by the average yield strength scaled according to the hybrid ratio.

to but does not coincide with the optimal transition points. Note that these curves are located dimensionless. The minimum is located at the top of the graph, and the maximum at the bottom. Also, note that a fitted curve (continuous red curve) has been added to better reflect the behavior of the optimal cost as a function of the location of the transition point. The next option was to combine both internal forces. However, the values alone cannot be combined due to the difference in units (and scale). Therefore, it was decided to sum the curves normalized by averaging. Each point of the curve is divided by the average of all values. It returns a

dimensionless value that can be combined with the other curve to which the same procedure is applied. When both normalized curves are summed, the red dotted line is obtained. In this case, it was found that the maximum of this curve coincides almost entirely with the minimum of the fitted curve (black arrow). This minimum coincides with or is very close to the optimum transition point location. Therefore, it is concluded that the best practical position to make the transition (with two transition points) would be where the maximum of the curve formed by the normalized (by the mean) sum of the bending and shear

curves is located. Note that we are working with one-half of the element.

**3.2. Implementation of More Transition Points.** A fundamental aspect of including more transition points is where to place them. It must be done so that the longitudinal sections established take better advantage of the mechanical configuration (geometry + material) assigned to them. Figure 4 is presented to understand better this phenomenon of longitudinal hybridization with multiple transition points. The graphs represent all the optimal configurations for the 12 m girder under the three loading states. One of the aspects highlighted is the optimal position of the transition points according to each configuration. Note how the ordinate axis represents a somewhat abstract concept intended to show the material configurations obtained for each section. A good representation could be the mean between the two  $f_y$  values for flanges and web. However, this value alone would not fully account for the hybridization phenomenon. For this reason, we propose the mean multiplied by the hybrid ratio  $((f_{yw} + f_{yf})/2) \times R_h$ . It includes the average section quality in terms of material and the differences between the steels of the plates. We refer to this term as “scaled  $f_{y\_med}$ ”

Specific trends can be appreciated in the graphs of the figure. Regarding the position of the transition points, it can be seen how three common transition zones are defined in each case study for various configurations. It can be seen how the first common transition zone is quite similar for the three cases. Cases (b) and (c) also present a similar second zone. The third zone that can be discerned differs considerably from case to case. However, we attempt below to unify the criteria to provide general recommendations for establishing transitions.

As for the use of the material, note as in bottom graph the longitudinally homogeneous configuration presents a lower scaled  $f_{y\_med}$  value than other configurations of the element itself (plateau formed between 1.75 and 4.20 approximately). This value is also visibly lower than the other two case studies. It is due to the limitation set by the upper limit for  $h_w$ , so the algorithm cannot search for a mechanical configuration like the previous cases. In other words, not only is the optimal geometric configuration affected but also the hybridization phenomenon cannot be developed in its whole dimension. Note how the web steel (550 MPa) is better quality than in the other two cases (355 and 450 MPa) to deal with higher stresses with a less efficient geometrical distribution.

One of the main unknowns and the main contribution of this research is to check the efficacy of longitudinal hybridization. It also means observing the element’s behavior in function of the number of cuts or transitions implemented. Figure 5 shows what happens to the cost of each optimal solution as a function of the number of transition points. It can be appreciated that, as predicted in the previous section, implementing more than two transitions increases the economic efficiency of the element. It can also be checked how implementing TLH girders is more effective as the element is more stressed. Another important conclusion is that implementing more than six transition points is ineffective since

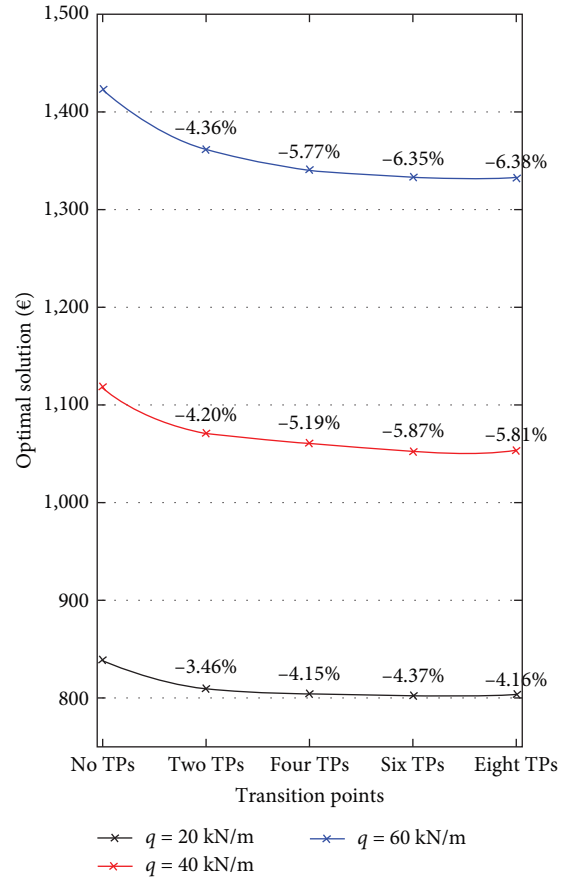


FIGURE 5: Influence of the number of transition points on the optimum cost and comparison (in percentage) with the transversely hybrid element. Girder of 12 m.

the indexes worsen or the improvement is insignificant. It also increases the constructive complexity of the structure.

**3.3. Optimization of Other Girders.** Once the optimization strategies for establishing TLH configurations have been tested and validated, it is time to apply them to other case studies. Using the 12 m girder with three different load states as case studies has yielded some interesting results. Two additional 16 and 20 m elements are used to validate the proposed strategies with the same three load cases.

Figure 6 shows the results of optimizing the three elements with the three load states implementing the four proposed TLH configurations. The figure shows that the highest savings concerning the longitudinally homogeneous configuration are obtained for the 20 m girder (lower graph). On the other hand, the 16 m one obtains more dispersed results, with a broader range of minimum and maximum savings (middle graph). Finally, the 12 m element shows similar savings to the 16 m one but with more stability (upper graph).

This figure also shows the optimum transition positions for each configuration and each loading state. For example, if it is wanted to know the optimum positioning of the transition points on the 20 m girder for a six TPs configuration and a load of 60 kN/m, just look for the red circles in the lower graph of the figure. The position of the three transition

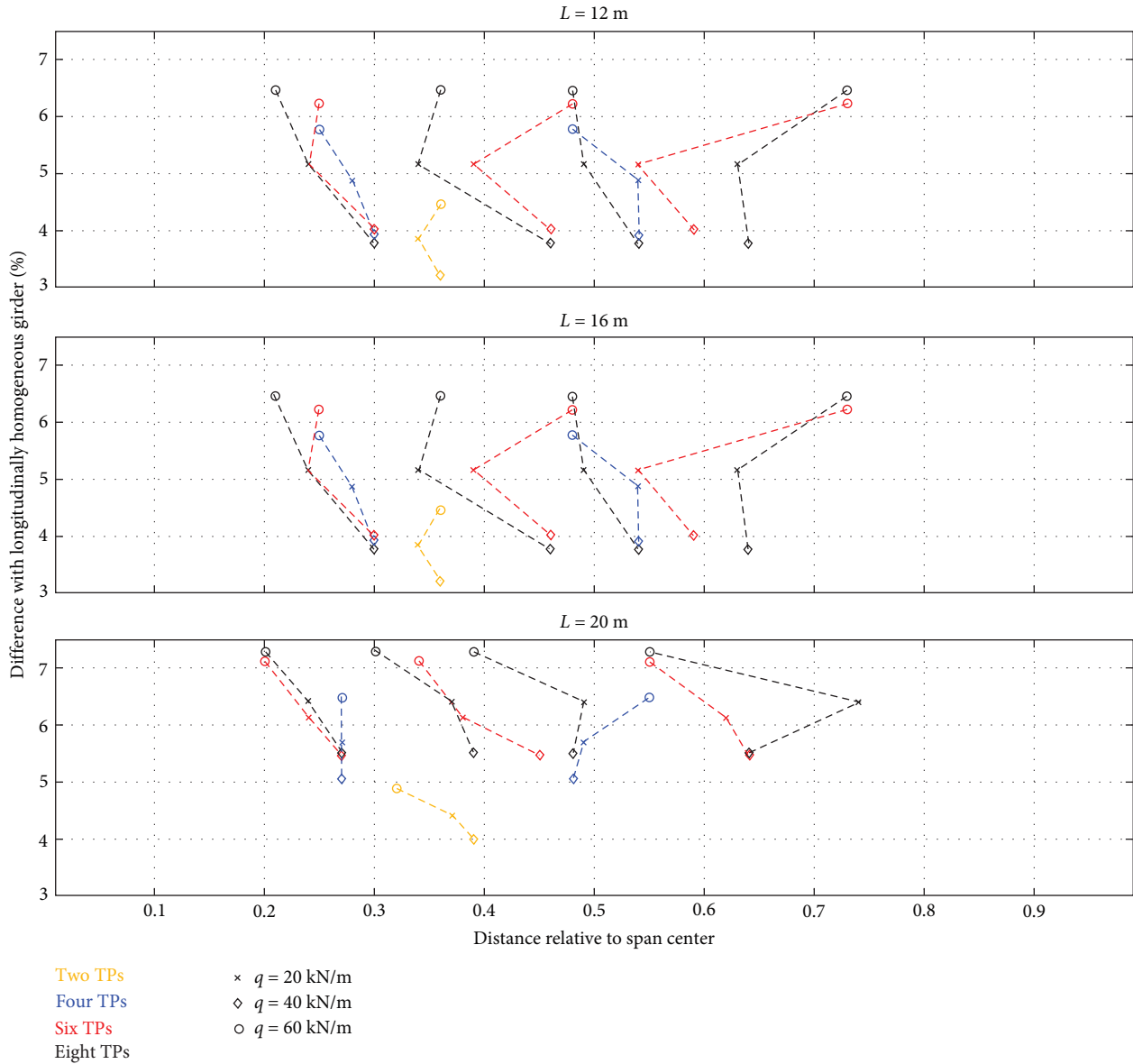


FIGURE 6: Optimal position of the transition points for each case study and percentage difference of each configuration regarding its longitudinally homogeneous counterpart.

points concerning the center of the span would be 0.20, 0.34, and 0.55, with a saving of 7.12% with respect to the longitudinally homogeneous configuration. Note that each transition point of each loading state is joined with a dashed line to highlight the relative positioning of each configuration as a function of how stressed the element is. Here it can be seen that the girders subjected to the highest load benefit best from longitudinal hybridization. The exception is in the 16 m element, where more benefits are obtained for the 20 kN/m load than for the 40 kN/m one.

These graphs also show similarities in positioning the transition points for each configuration. For example, to set two TPs, they should be symmetrically placed between 30% and 40% of half the span. For more than two points, the first cut should generally be made about 20% of half the length, and similar.

This figure also reaffirms the conclusions of Figure 5 on the number of recommended TPs. Here it can be seen that establishing six transition points in many cases is more beneficial than eight, and in the opposite case, the difference is minimal. However, if establishing this configuration of six transitions could lead to a technological or other (e.g., structural) problem, some recommendations are proposed for where to place the transition points for more straightforward configurations. For two TPs, it was already mentioned that the position should be between 0.30 and 0.40 times half the length of the element. By calculating this point as the maximum of the sum of the normalized moment and shear plots, effectively, the optimal transition position is 0.35 half the length. For four TPs and  $L = 12\text{ m}$ , the first cutoff point is at an average length of 0.24 times half the span, while the second is at 0.53. For  $L = 16\text{ m}$ , the points would be at 0.28

TABLE 1: Optimal configurations of each case study implementing six TPs.

Config.	Geometric variables (mm)				TPs position*			Material configuration ( $f_{yw}$ - $f_{yf}$ , MPa)			
	$h_w$	$t_w$	$b_f$	$t_f$	First	Second	Third	First**	Second	Third	Center
C1	850	5	120	12	0.25	0.40	0.54	235–235	235–420	275–550	355–700
C2	990	5	170	12	0.18	0.31	0.54	235–235	235–450	355–700	450–890
C3	1,000	5	550	6	0.19	0.36	0.70	235–235	235–450	355–700	550–700
C4	1,120	5	170	12	0.24	0.39	0.54	235–235	235–420	275–550	355–700
C5	1,470	5	740	5	0.30	0.46	0.59	235–235	235–355	235–450	275–550
C6	1,490	6	770	5	0.25	0.48	0.73	235–275	275–550	355–700	450–700
C7	1,500	5	160	14	0.24	0.38	0.62	235–235	235–450	355–600	420–700
C8	1,690	6	860	5	0.27	0.45	0.64	235–235	235–420	275–550	355–600
C9	1,660	8	890	5	0.20	0.34	0.55	235–235	275–450	355–700	450–890

\*Distance relative to center span. \*\*Extreme configuration.

and 0.52, respectively. For  $L = 20$  m, the distribution would be 0.27 and 0.51, respectively. It is concluded that to apply four TPs, the first point should be placed at an average position of  $0.26(L/2)$ , while the second would be at  $0.52(L/2)$ . As for the recommended configuration (six TPs), the three transitions for  $L = 12$  m should be made at 0.21, 0.36, and 0.59 of half the length. For  $L = 16$  would be 0.26, 0.49, and 0.62. For  $L = 20$  m, the distribution would be 0.24, 0.39, and 0.60. Therefore, for six TPs, it is recommended to make the transitions by 0.24, 0.40, and 0.60 times half the element length. Note how for four and six TPs, the first cut point coincides quite well, as previously mentioned.

Another recommendation of relevant importance would be which steel configurations to use. For two TPs, the extreme configuration always remains with the lower quality steel in the web (S235). For the flanges, it is recommended to use S355 steel for less stressed elements ( $R_h = 1.51$ ) and S450 for elements subjected to higher loads ( $R_h = 1.91$ ). In the case of the central configuration, the most used steel in the web is S355, while in the flanges, it is S700 ( $R_h = 1.97$ ). Other alternatives can be implemented depending on how stressed the element is, always trying to obtain the highest possible  $R_h$  within the admissible ( $\leq 2$ ). Note that steels higher than S700 are rarely selected within the optimum configurations (S890 only twice).

For configurations with four TPs, the extreme section is always composed of S235 steel in the web. The flange steel is sometimes composed of the same steel (homogeneous section), especially for elements of shorter length and lower load. The most frequently repeated configuration is with S275 steel ( $R_h = 1.17$ ). Sections are also obtained with S355 steel flanges ( $R_h = 1.51$ ). For the second configuration, the most used steel in the web is S275, combined with mainly S500 flanges ( $R_h = 1.82$ ). If the element has considerable length or loads, the flange steel could be increased to S550 ( $R_h = 1.51$ ), or even increase the web and flange steel while maintaining similar hybrid ratios. The central configuration is the same as for the other elements. Recall that it has been found that the center section for TLH girders is the same as that obtained by optimizing the element only with transversal hybridization.

As for the elements subject to the recommended configuration (six TPs, Table 1), the extreme section is usually homogeneous and made up of the lower quality steel. The second span generally consists of S235 web steel combined with S420 ( $R_h = 1.79$ ) or S450 ( $R_h = 1.91$ ) steel for the flanges. For the third span, the common option is to use S355 steel for the web, with S700 being the most combined steel for the flanges ( $R_h = 1.97$ ). However, since this is the recommended configuration for the central section, lower average quality variants (e.g., S355–S500, S355–S550) could be sought. In cases where it is mandatory to establish this combination in the third section, the central section will require combinations with higher quality steels, as shown in Table 1.

Once it was determined that establishing eight transitions would not be advisable, six TPs will be implemented in each case study for longitudinal hybridization. It aims to compare the results of building TLH girders with only transversely hybrid and traditional homogeneous ones. Figure 7 shows the cost differences between the hybrid girders and traditional elements. Note that all designs are optimized in terms of cross-section geometry. That is, the geometric configurations are optimal in each case. The material distribution is what varies.

The figure shows a trend already discussed: the greater effectiveness of transverse hybridization for elements with smaller spans. There is the exception of C3 ( $L = 12$  m,  $q = 60$  kN/m), where the  $h_w$  parameter upper constraint of the section does not allow full development of transverse hybridization. In contrast, longitudinal hybridization is more effective for longer spans. It is proven by the results shown above and can be seen in the figure by the greater distance between the thin and the thick line for elements of greater length. The total savings achieved for cases C1, C2, and C9 are outstanding, with more than 13% of difference. In general, it can be established that the TLH elements save, on average, about 10% in manufacturing costs compared to their homogeneous counterparts.

Table 1 shows the optimal TLH configurations (geometry and material) for the case study. A side view of the case study (C1) is shown in Figure 8. Here it can be seen how the hybrid configurations would look compared to the homogeneous one. In addition, the total manufacturing costs and the

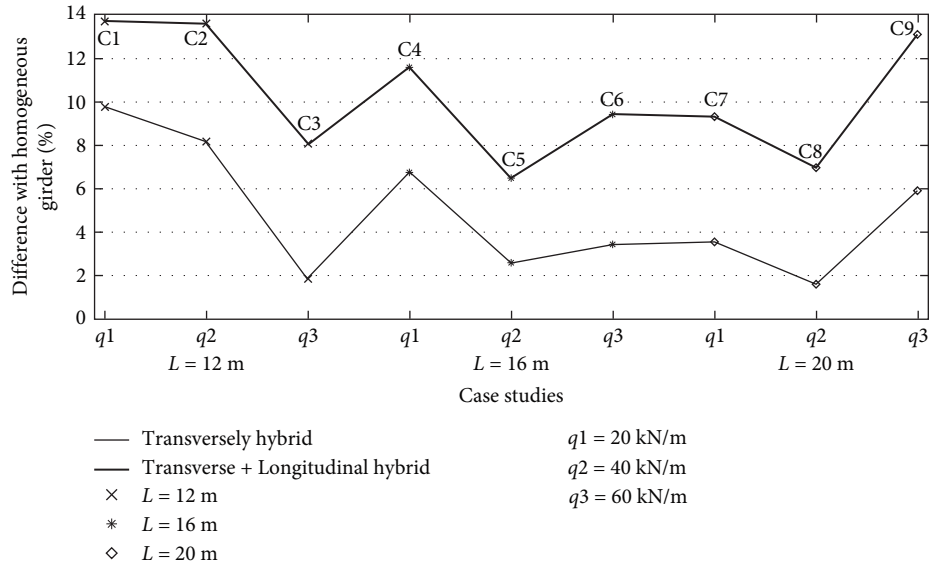


FIGURE 7: Percentage savings for each case study with both hybrid configurations (transverse only and TLH) with respect to their homogeneous counterparts.

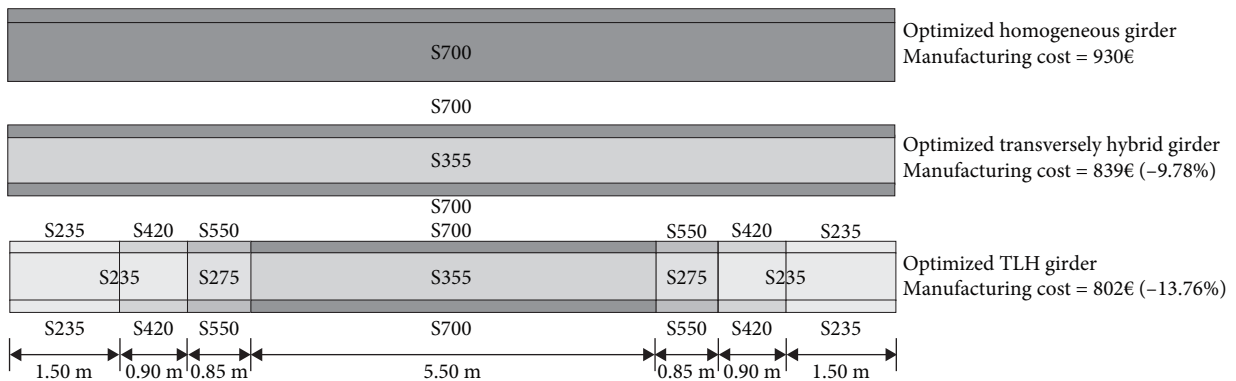


FIGURE 8: Side view of C1 to understand better the transverse–longitudinal hybridization phenomenon.

corresponding savings are shown. It should be noted that the section dimensions ( $h_w, t_f$ ) are not to scale. Even an exaggerated representation of  $t_f$  is made to visualize better the colors representing the different steel grades. On the other hand, the longitudinal dimensions are to scale to understand better how a TLH-configured element would be distributed.

3.3.1. *Application of Practical Recommendations.* To apply the practical recommendations generated and generalize the results, a new case study is used (girder of  $L=18$  m,  $q=40$  kN/m). The aim is to demonstrate the applicability of hybridization (both longitudinal and transverse) to improve the economic indexes of the studied elements. In addition, the results of a traditional design are compared with those obtained using an optimization algorithm as the basis for the design. That is why the first methodology (D1) has a traditional approach. It is used modeling, analysis, and structural design software (SAP2000). The design is performed by selecting from a list of real I-section the one with the lowest weight that complies with the design constraints. In this case,

the selected cross-section is W40x221 (AISC catalog). The dimensions of this profile are adapted to the values allowed in this study, and the element is checked using the programmed algorithm. The steel selected is the reference one (S355). The dimensions are shown in Table 2. The second design approach (D2) consists of optimizing the homogeneous element. Here, the type of steel used throughout the element is optimized in addition to the cross-section geometry. As for the hybrid elements, the first design (D3) is the element with a hybrid configuration only transversely. The following designs allow longitudinal hybrid configuration with two (D4), four (D5), six (D6), and eight (D7) transition points. Note that the cross-section dimensions are optimized in all cases (except D1). Recall also that designs 3, 4, 5, 6, and 7 use the same geometrical configuration of the section. Here, the TLH configurations are established manually, following the recommendations provided. It validates their use and ratifies their influence on improving the economic indexes. Table 2 shows the material configurations implemented according to the recommendations. The transition

TABLE 2: Configuration and differences in manufacturing cost of the test case study ( $L = 18$  m,  $q = 40$  kN/m) using different design approaches (Ds).

Config.	Geom. variables (mm)			$t_f$	$t_f$	Material configuration ( $f_{yw}$ - $f_{yp}$ MPa)					Cost (€)	Saving (%) <sup>†</sup>	Saving (%) <sup>††</sup>
	$h_w$	$t_w$	$b_f$			First*	Second	Third	Fourth	Center			
D1	950	18	450	—	25	—	—	—	—	355–355	5,046	—	—
D2	1,540	6	210	—	14	—	—	—	—	700–700	2,619	48.10	—
D3	1,610	6	260	—	14	—	—	—	—	355–700	2,480	50.85	5.31
D4	1,610	6	260	235–420	14	—	—	—	—	355–700	2,388	52.68	8.82
D5	1,610	6	260	235–275	14	275–550	—	—	—	355–700	2,351	53.41	10.23
D6	1,610	6	260	235–235	14	235–450	355–550	—	—	355–700	2,341	53.61	10.61
D7	1,610	6	260	235–235	14	235–275	235–450	355–550	—	355–700	2,347	53.49	10.39

D1: traditional design; D2: optimized homogeneous girder; D3: optimized transversely hybrid girder; D4: optimized TLH girder with two TPs; D5: optimized TLH girder with four TPs; optimized D6: TLH girder with six TPs; optimized D7: TLH girder with eight TPs. Longitudinal hybridization in D4, D5, D6, and D7 is applied according to the established recommendations. \* Extreme configuration, † compared to traditional design, and †† compared to optimized homogeneous girder.

points for each configuration are also applied where recommended in the previous section.

Table 2 shows, in the first instance, the superiority of applying design optimization procedures over traditional methods. Notice how the improvements range from 48.10% to 53.49%. The other central point to highlight is the confirmation of the TLH configurations as more economically efficient than the homogeneous and the transversely hybrid elements. The latter improves the economic indexes of the homogeneous by 5.31%. Concerning the TLH girders, it can be seen how the configuration with six TPs is confirmed as the most efficient, improving the homogeneous and transversely hybrid designs by 10.61% and 5.60%, respectively. Remember that these improvements have been achieved only by following the established recommendations.

As it has been appreciated, the proposed methodology has allowed us to explore and exploit the benefits of hybrid construction. The practical implications of this proposal in the construction industry and the design of structures such as bridges and buildings are palpable. Its application can be extended either by formulating the design problem as an optimization one according to the described strategy, or by applying the recommendations established as a consequence of the results analysis.

Using both approaches, economic (and, by extension, environmental) indexes can be improved by up to 50% compared to traditional profiles and up to 15% compared to geometrically optimized but homogeneous structures. For its part, longitudinally hybrid construction can benefit elements with longer spans, such as bridges. In addition, the proposed methodology is the basis for exploring other alternatives in the optimal mechanical design of this type of structure. Instead of varying only the material in the longitudinal direction, the geometric component could also be given freedom, possibly achieving even more efficient typologies such as hybrid tapered girders. However, studying and developing efficient connections to achieve this type of typology is a field that needs special attention.

*3.4. Some Comments on Future Research.* Having proven that the construction of welded plate girders with hybrid transverse and longitudinal configurations offers considerable economic benefits over their homogeneous counterparts, it would be prudent to investigate the structural behavior of these elements further. It is accomplished with experimental work in the laboratory. It should be emphasized that most steel element design standards do not explicitly present rules for working with hybrid elements. Therefore, because of practical experimentation, it is necessary to be more explanatory in the standards about the procedure and particularities of the design of hybrid steel structures.

Another aspect to highlight for future work is the implementation of other types of support conditions. In this research, the girder is considered as simply supported. Another type of support would drastically change the distribution of internal forces and, with this, the hybrid configurations. In addition, the use of this type of construction should be examined in elements of greater length. The next step would be to optimize the design of these elements as part

of the structural assembly (e.g., steel box girders). Optimization of the whole assembly, including other design variables, would be very beneficial. For example, in a steel–concrete composite bridge, variables could be set to allow the use of hybrid configurations in the steel elements and, at the same time, optimize the design of the concrete elements. It also allows consider the interrelation between elements, since the presence of a concrete slab is beneficial for the stiffness of the girder, and therefore, of the whole assembly. Another aspect proven in this and previous research is the efficiency of hybridization for elements with small spans. It opens the possibility of studying and using steel girders with hybrid configurations in buildings. A further important application would be to vary not only the configuration of the material along its length but also the geometry. It would result in obtaining hybrid girders of variable cross-sections (tapered girders).

An alternative aspect that could be studied in depth is the joints to guarantee the longitudinally hybrid element. Other variants could be explored to ensure more efficient connections (e.g., bolted). What is essential in optimizing the design of these elements is the ratio of the cost of the joint to the total cost. The more the joint costs to build, the less effective the longitudinal hybridization will be. Therefore, other types of connections, such as bolted ones, which are even cheaper to implement, would further enhance the value of this strategy of constructing longitudinally hybrid elements.

Finally, an additional critical point for future research development in this field is focused on the formulation of the problem and the way to solve it. Sustainability is defined by four other criteria besides economic: environmental, social, durability, and buildability. It means that problems must be formulated with a more comprehensive approach. Moreover, the focus should not be limited only to the design stage. The entire life cycle of the structure must be addressed, including very influential stages such as the maintenance of the structure. All this turns, the problem more challenging, making it necessary to explore multiobjective optimization alternatives. It, in turn, means implementing multicriteria decision-making strategies. By unifying all these branches, it will be possible to obtain more sustainable designs, which is much needed in the construction sector worldwide.

## 4. Concluding Remarks

This study explores the possibility of establishing hybridization in the longitudinal direction of welded I-section plate girders. Previous studies have demonstrated the economic advantages of using different steel grades in the flanges and web (transverse hybridization). Still, the possibility of establishing differences in the longitudinal direction has yet to be explored. For this, mathematical optimization methods are used that search for the optimal mechanical configuration by allowing different types of steel in the transverse plane and by making it possible to establish different types of sections in terms of material along the structure. The objective function is the manufacturing cost, which includes seven other activities, such as welding or painting, besides the material



cost. The constraints are based on compliance with Eurocode 3 specifications.

The results show that building transverse and longitudinally hybrid (TLH) elements is beneficial from a sustainability point of view. The recommended configuration establishes six transition points, which means one element with four types of hybrid sections symmetrically located. Unlike longitudinal hybridization, which is more efficient as the girder span is smaller, TLH configurations demonstrate more effectiveness as the element length increases. In general, to implement two transitions, it is recommended that the transition be located at approximately 0.35 half of the length  $L$  ( $0.35 * L/2$ ). The extreme configuration alternates between S235–S355 (web steel-flanges steel) for less stressed elements and S235–S450 for more stressed ones. The central configuration would be S355–S700. To establish typologies with four transitions, the first should be located at  $0.26 * L/2$  and the second at  $0.52 * L/2$ . The extreme configuration would be S235–S275, the second alternating between S275–S500 for less loaded elements or S275–S550 otherwise. The central configuration would remain S355–S700. For the most economically efficient typology (six transitions), the first transition should be located at  $0.24 * L/2$ , the second at  $0.40L/2$ , and the third at  $0.60 * L/2$ . The external configuration would be homogeneous (S235–S235), the second S235–S420 for less stressed elements and S235–S450 for more stressed ones, and the third S355–S500 for the first case and S355–S550 for the second, while the central one would be the same as the previous typologies (S355–S700).

In an experiment using the various practical recommendations derived from the results, it is observed that this novel practice improves the economic indexes by more than 50% compared to a structure designed with the traditional method and by more than 10% compared to an optimized structure with homogeneous configuration. Therefore, the proposed methodology is the basis for studying new typologies based on transversal and longitudinal mechanical freedom (geometry + material) to seek more sustainable configurations than those implemented in traditional design.

Even so, specific gaps in knowledge need to be filled. That is why several future lines of research are proposed. Among the most important aspects are to develop more practical work in the laboratory to deepen the structural behavior of both transverse hybrid and TLH girders. Of the latter, one aspect that should be dealt with in depth would be the issue of joints. Another important aspect lies in the formulation of the optimization problem. Other criteria besides the economic one should be implemented, i.e., environmental, social, durability, and buildability. In addition, the approach should go beyond the design stage, considering the structure's life cycle. Finally, the proposed methodology should be extended to other structures, such as TLH girders with variable cross-sections, or more complex ones such as box girders.

## Nomenclature

$A_{fc}$ :	Effective cross-area of the compression flange
$B$ :	Vector containing the possible values of the variables related to width of plates

$b_f$ :	Width of both flanges
$C_B(\mathbf{X})$ :	Blasting cost
$C_C(\mathbf{X})$ :	Cutting cost
$C_E(\mathbf{X})$ :	Erecting cost
$C_J(\mathbf{X})$ :	Cost of the joints
$C_M(\mathbf{X})$ :	Material cost
$C_P(\mathbf{X})$ :	Painting cost
$C_S(\mathbf{X})$ :	Sawing cost
$C_T(\mathbf{X})$ :	Transportation cost
$C_W(\mathbf{X})$ :	Welding cost
$E$ :	Modulus of elasticity of steel
$f_y$ :	Nominal yield strength of steel
$f_{yf}$ :	Nominal yield strength of flanges steel
$f_{yw}$ :	Nominal yield strength of web steel
$h_w$ :	Web height
$I_y$ :	Inertia of the cross-section with respect to the bending axis
$k$ :	Coefficient to regulate the flange buckling against web
$L$ :	Overall length of the girder
$M$ :	Vector containing the possible values of the variables related to steel quality
$M_{cr}$ :	Critical bending moment calculated with the gross cross-section properties
$M_{Ed}$ :	Maximum acting bending moment
$M_{Rk}(\mathbf{X})$ :	Bending resistance of the section
$M(\mathbf{X})$ :	Material cost of the girder
$q$ :	Uniform load applied to the girder
$q_{SLS}$ :	Serviceability limit state load
$q_T$ :	Total uniform load acting on the girder
$R_h$ :	Hybrid ratio
$T$ :	Vector containing the possible values of the variables related to thickness of plates
$t$ :	Thickness of the plate
$f$ :	Flanges thickness
$t_w$ :	Web thickness
TLH:	Transverse–longitudinal hybridization
TPs:	Transition points
$\bar{u}$ :	Maximum allowed displacement
$u_{\max}(\mathbf{X})$ :	Maximum displacement of the girder
$V_{c,Rd}(\mathbf{X})$ :	Plastic shear resistance of the girder
$V_{Ed}$ :	Maximum acting shear force
$x_i$ :	Position of the transition points
$\lambda_{LT}$ :	Slenderness parameter of a section
$\eta$ :	Parameter for regulating the shear resistance.

## Data Availability

The data used to support the conclusions of this study are available from the corresponding author upon request.

## Conflicts of Interest

The authors declare that they have no conflicts of interest.

## Acknowledgments

This work was supported by the grant PID2020-117056RB-I00, which was funded by MCIN/AEI and by ERDF A way of

making Europe and grant PRE2021-097197 funded by MCIN/AEI and FSE+. Open access funding enabled and organized by CRUE-UNIRIS 2024.

## References

- [1] L.-Y. Shen, W.-S. Lu, H. Yao, and D.-H. Wu, "A computer-based scoring method for measuring the environmental performance of construction activities," *Automation in Construction*, vol. 14, no. 3, pp. 297–309, 2005.
- [2] T. Ramesh, R. Prakash, and K. K. Shukla, "Life cycle energy analysis of buildings: an overview," *Energy and Buildings*, vol. 42, no. 10, pp. 1592–1600, 2010.
- [3] I. J. Navarro, V. D. Yepes, J. V. Martí, and F. González-Vidosa, "Life cycle impact assessment of corrosion preventive designs applied to prestressed concrete bridge decks," *Journal of Cleaner Production*, vol. 196, pp. 698–713, 2018.
- [4] United Nations, "Sustainable development goals, sustainable cities and communities," <https://www.un.org/sustainabledevelopment/cities/>.
- [5] P. M. Martínez Fernández, I. Villalba Sanchís, V. Yepes, and R. Insa Franco, "A review of modelling and optimisation methods applied to railways energy consumption," *Journal of Cleaner Production*, vol. 222, pp. 153–162, 2019.
- [6] I. J. Navarro, V. Yepes, and J. V. Martí, "Social life cycle assessment of concrete bridge decks exposed to aggressive environments," *Environmental Impact Assessment Review*, vol. 72, pp. 50–63, 2018.
- [7] W. Choi, Y. Choi, and S.-W. Yoo, "Flexural design and analysis of composite beams with inverted-t steel girder with ultrahigh performance concrete slab," *Advances in Civil Engineering*, vol. 2018, Article ID 1356027, 16 pages, 2018.
- [8] Z. Zhang, Y. Liu, B. Feng, Y. Ma, and G. Zhang, "Analytical solutions for girder distribution factor in steel–concrete composite girders with the effect of parapets," *Advances in Civil Engineering*, vol. 2021, Article ID 8471801, 19 pages, 2021.
- [9] A. El-Zohairy, S. Mustafa, H. Shaaban, H. Salim, and A. A. Allawi, "Numerical modeling and analysis of strengthened steel–concrete composite beams in sagging and hogging moment regions," *CivilEng*, vol. 4, no. 2, pp. 483–505, 2023.
- [10] A. Terreros-Bedoya, I. Negrin, I. Payá-Zaforteza, and V. Yepes, "Hybrid steel girders: review, advantages and new horizons in research and applications," *Journal of Constructional Steel Research*, vol. 207, Article ID 107976, 2023.
- [11] O. Skoglund, J. Leander, and R. Karoumi, "Optimizing the steel girders in a high strength steel composite bridge," *Engineering Structures*, vol. 221, Article ID 110981, 2020.
- [12] ANSI/AISC 360-16, "Specification for Structural Steel Buildings," American Institute of Steel Construction, 2016.
- [13] AASHTO, "AASHTO LRFD Bridge Design Specifications," American Association of State Highway and Transportation Officials, Washington, D.C., 2010.
- [14] G. P. Wollmann, "Steel girder design per AASHTO LRFD specifications (part 1)," *Journal of Bridge Engineering*, vol. 9, no. 4, 2004.
- [15] G. P. Wollmann, "Steel girder design per AASHTO LRFD specifications (part 2)," *Journal of Bridge Engineering*, vol. 9, no. 4, 2004.
- [16] EN 1993-1-5, "Eurocode 3: design of steel structures. Part 1–5: plated structural elements," CEN, 2006.
- [17] EN 1993-1-1, "Eurocode 3: design of steel structures. Part 1-1: general rules and rules for buildings," CEN, 2005.
- [18] M. Veljkovic and B. Johansson, "Design of hybrid steel girders," *Journal of Constructional Steel Research*, vol. 60, no. 3–5, pp. 535–547, 2004.
- [19] K. Mela and M. Heinisuo, "Weight and cost optimization of welded high strength steel beams," *Engineering Structures*, vol. 79, pp. 354–364, 2014.
- [20] I. Negrin, M. Kripka, and V. Yepes, "Design optimization of welded steel plate girders configured as a hybrid structure," *Journal of Constructional Steel Research*, vol. 211, Article ID 108131, 2023.
- [21] C. G. Schilling, "Web crippling tests on hybrid beams," *Journal of the Structural Division*, vol. 93, no. 1, pp. 59–70, 1967.
- [22] D. J. Fielding and A. A. Toprac, "Fatigue tests of hybrid plate girders under combined bending and shear," <http://library.ctr.utexas.edu/digitized/TexasArchive/phase1/96-2-CHR.pdf>.
- [23] P. S. Carskaddan, "Shear buckling of unstiffened hybrid beams," *Journal of the Structural Division*, vol. 94, no. 8, pp. 1965–1990, 1968.
- [24] A. Azizinamini, J. B. Hash, A. J. Yakel, and R. Farimani, "Shear capacity of hybrid plate girders," *Journal of Bridge Engineering*, vol. 12, no. 5, pp. 535–543, 2007.
- [25] M. Shokouhian and Y. Shi, "Flexural strength of hybrid steel I-beams based on slenderness," *Engineering Structures*, vol. 93, pp. 114–115, 2015.
- [26] C.-S. Wang, L. Duan, Y. F. Chen, and S.-C. Wang, "Flexural behavior and ductility of hybrid high performance steel I-girders," *Journal of Constructional Steel Research*, vol. 125, pp. 1–14, 2016.
- [27] Y. Zhu, X. Yun, and L. Gardner, "Behaviour and design of high strength steel homogeneous and hybrid welded I section beams," *Engineering Structures*, vol. 275, Article ID 115275, 2023.
- [28] D. Huang, X. Nie, J. Fan, and R. Ding, "Experimental study on longitudinal shear behavior of prefabricated steel–concrete composite beams with notched connections," *Engineering Structures*, vol. 300, Article ID 117151, 2024.
- [29] R. A. Bhat and L. M. Gupta, "Behaviour of hybrid steel beams with closely spaced web openings," *Asian Journal of Civil Engineering*, vol. 22, no. 1, pp. 93–100, 2021.
- [30] G. N. Narule, S. G. Morkhade, and S. R. Kumbhar, "Analytical behavior of steel hybrid girder with opening in web," in *Proceedings of the Indian Structural Steel Conference 2020*, M. Madhavan, J. S. Davidson, and N. E. Shanmugam, Eds., vol. 1 of *ISSC 2020. Lecture Notes in Civil Engineering*, Springer, Singapore.
- [31] M. Bock, M. Gkantou, M. Theofanous, S. Afshan, and H. Yuan, "Ultimate behaviour of hybrid stainless steel cross-sections," *Journal of Constructional Steel Research*, vol. 210, Article ID 108081, 2023.
- [32] S. Zha, D. Liu, J. Zhang, W. Deng, and J. Gu, "Calculation method for flexural capacity of composite girders with corrugated steel webs," *Journal of Constructional Steel Research*, vol. 214, Article ID 108476, 2024.
- [33] M. A. El-Aghoury, A. M. Ebid, and K. C. Onyelowe, "Optimum design of fully composite, unstiffened, built-up, hybrid steel girder using GRG, NLR, and ANN techniques," *Journal of Engineering*, vol. 2022, Article ID 7439828, 25 pages, 2022.
- [34] V. S. Ronanki, S. Aaleti, and J. P. Binard, "Long-span hybrid precast concrete bridge girder using ultra-high-performance concrete and normalweight concrete," *PCI Journal*, vol. 64, no. 6, pp. 45–61, 2019.

- [35] Y. Li, Y. Lai, G. Lu, F. Yan, P. Wei, and Y. M. Xie, "Innovative design of long-span steel–concrete composite bridge using multi-material topology optimization," *Engineering Structures*, vol. 269, Article ID 114838, 2022.
- [36] Z.-Q. He, J. Chen, Z. Liu, and Z. J. Ma, "An explicit approach for determining the rational length of steel portion in steel–concrete hybrid girder bridges," *Journal of Bridge Engineering*, vol. 28, no. 1, Article ID 05022011, 2023.
- [37] B. Shangguan, Q. Su, J. R. Casas, H. Su, S. Wang, and R. Zhao, "Modeling and testing of a composite steel–concrete joint for hybrid girder bridges," *Materials*, vol. 16, no. 8, Article ID 3265, 2023.
- [38] J. F. Choo, Y. C. Choi, W. C. Choi, and S. W. Yoo, "Behavioral characteristics of hybrid girders according to type of steel–concrete connection," *Archives of Civil and Mechanical Engineering*, vol. 19, no. 1, pp. 47–62, 2019.
- [39] S.-H. Kim, C.-G. Lee, J.-H. Ahn, and J.-H. Won, "Experimental study on joint of spliced steel–PSC hybrid girder, Part I: proposed parallel-perfobond-rib-type joint," *Engineering Structures*, vol. 33, no. 8, pp. 2382–2397, 2011.
- [40] S.-H. Kim, C.-G. Lee, S.-J. Kim, and J.-H. Won, "Experimental study on joint of spliced steel–PSC hybrid girder, part II: full-scale test of spliced hybrid I-girder," *Engineering Structures*, vol. 33, no. 9, pp. 2668–2682, 2011.
- [41] L. Zhao, G. Pu, Y. Yuan, Q. Guo, and Y. Yu, "Mechanical behaviour of steel–concrete joint in hybrid girder cable-stayed bridge," *Structures*, vol. 57, Article ID 105239, 2023.
- [42] Z. Wang, B. Li, P. Liu, Z. Wang, and S. He, "Evaluation of structural performance of steel–concrete joints in hybrid girder bridges," *Vibroengineering Procedia*, vol. 47, pp. 29–34, 2022.
- [43] I. Negrin, M. Kripka, and V. Yepes, "Multi-criteria optimization for sustainability-based design of reinforced concrete frame buildings," *Journal of Cleaner Production*, vol. 425, Article ID 139115, 2023.
- [44] V. Yepes and J. Medina, "Economic heuristic optimization for heterogeneous fleet VRPHESTW," *Journal of Transportation Engineering*, vol. 132, no. 4, pp. 303–311, 2006.
- [45] M. Veljkovic and B. Johansson, "Design for buckling of plates due to direct stress," in *NSCC 2001 Proceedings*, pp. 729–736, Helsinki University of Technology, 2001.
- [46] D. Simon, "Biogeography-based optimization," *IEEE Transactions on Evolutionary Computation*, vol. 12, no. 6, pp. 702–713, 2008.
- [47] I. Negrin, D. Roose, E. Chagoyén, and G. Lombaert, "Biogeography-based optimization of RC structures including static soil–structure interaction," *Structural Engineering and Mechanics*, vol. 80, no. 3, pp. 285–300, 2021.
- [48] I. Payá-Zaforteza, V. Yepes, F. González-Vidosa, and A. Hospitaler, "On the Weibull cost estimation of building frames designed by simulated annealing," *Meccanica*, vol. 45, no. 5, pp. 693–704, 2010.